Supplementary Figure 1

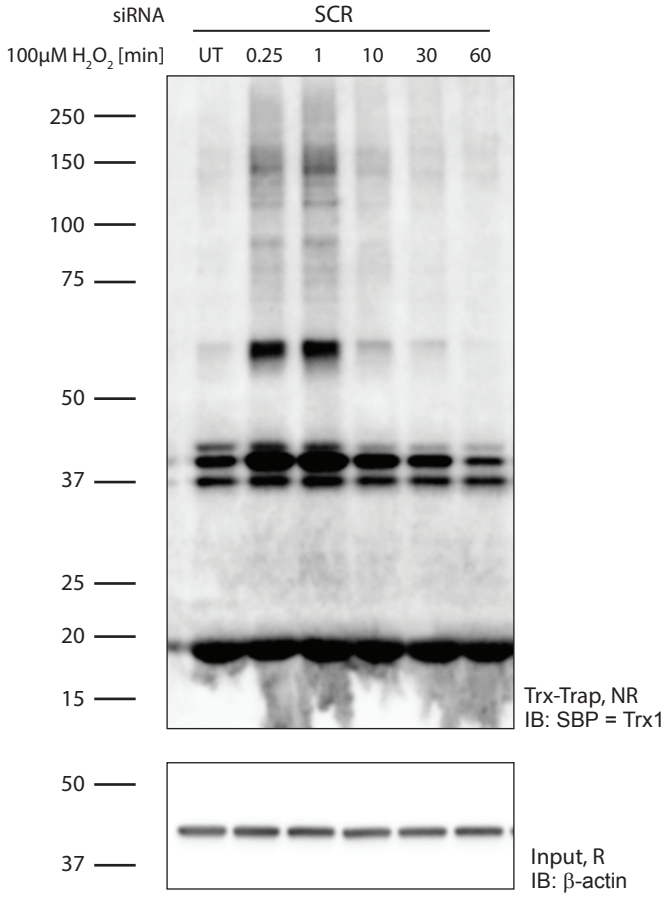

Supplementary Figure 1 | Protein thiol oxidation induced by 15 sec H_2O_2 bolus treatment is short-lived and fully reversible. Kinetic trapping time course in response to a 15 sec 100 μM H_2O_2 bolus treatment of wildtype HEK cells. IB = immunoblot; NR = non-reducing; R = reducing. Blots are representative of 2 independent experiments.

Supplementary Figure 2

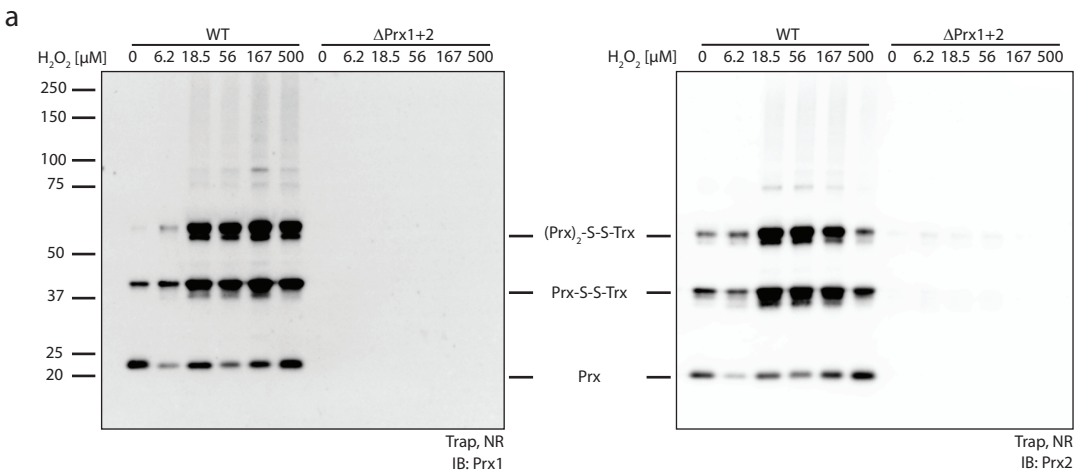

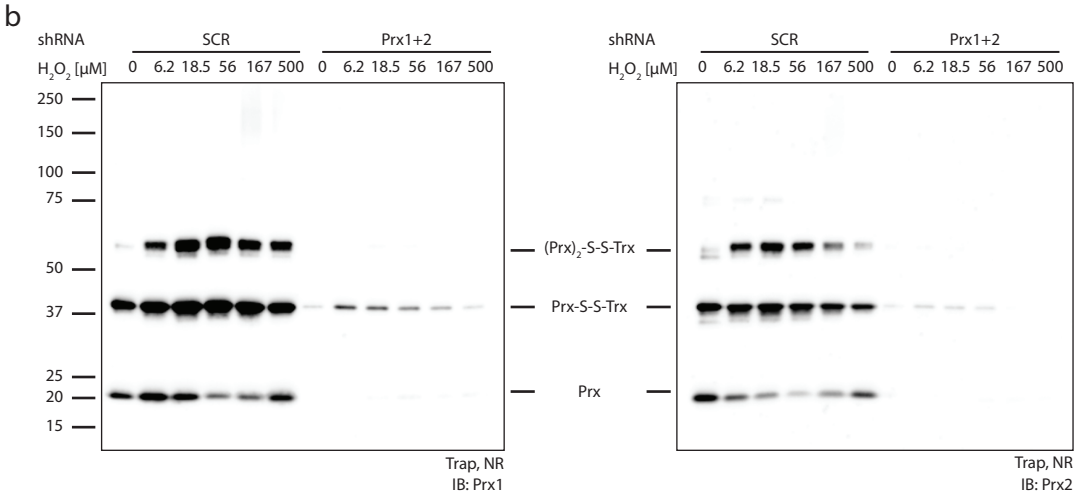

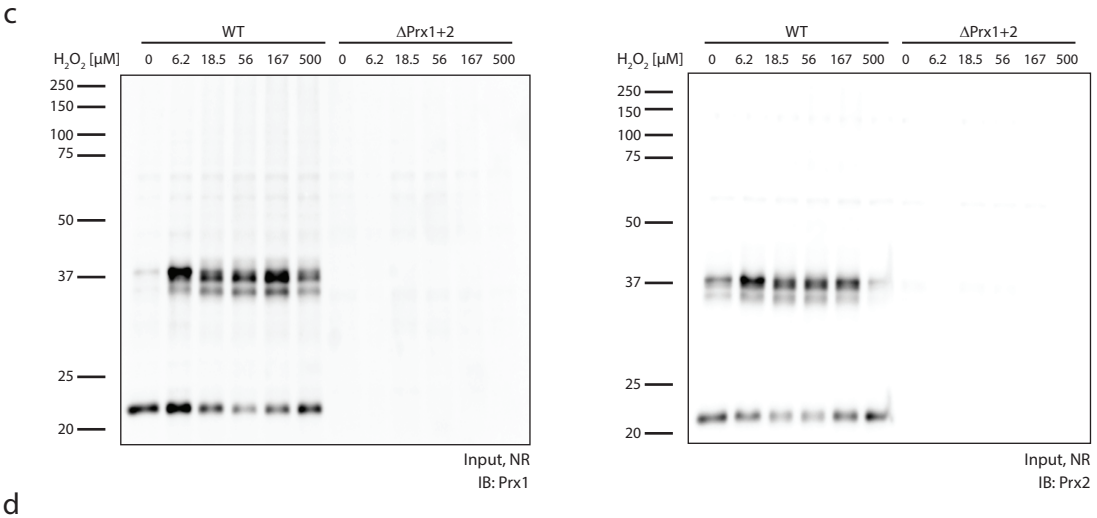

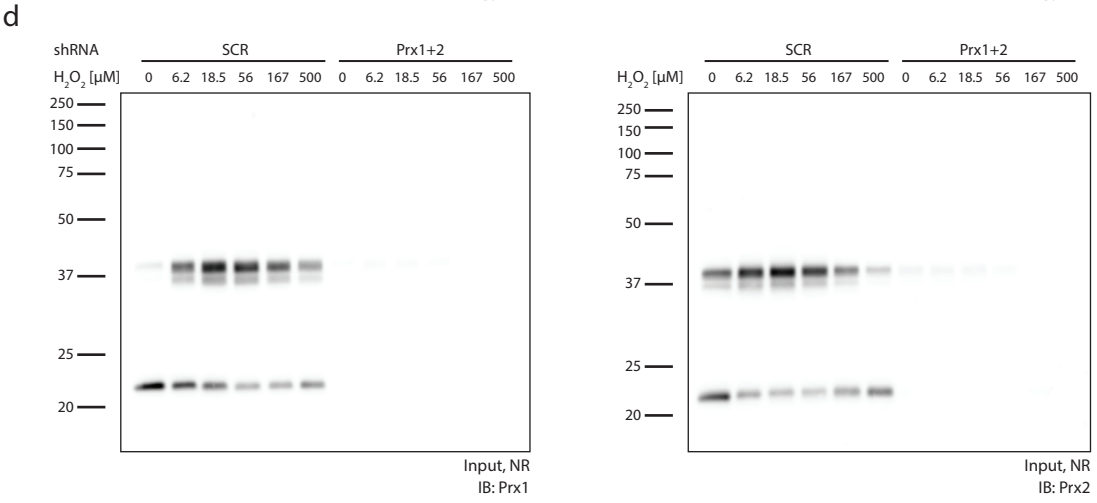

Nature Chemical Biology: doi:10.1038/nchembio.2536

Supplementary Figure 2 | Control blots relating to main figure 1c-d. (**a-b**) The material analyzed in main figure 1c-d (i.e. Trx(C35S) conjugates eluted from SA beads with biotin) was immunoblotted for Prx1 (left panels) and Prx2 (right panels). The result confirms the complete absence of both Prx1 and Prx2 in HAP1 double KO cells (**a**) and the almost complete depletion of Prx1 and Prx2 in HEK293T cells (**b**). The observed Prx immunoreactivity pattern confirms the identity of the major bands, as assigned in main figure 1 and above. It further confirms that the higher molecular weight bands induced by H_2O_2, as seen in main figure 1c-d (labelled 'Trx-S-S-X') are not Trx-Prx disulfide conjugates of higher stoichiometry, but primarily represent Trx(C35S) molecules conjugated to other proteins (as confirmed in later experiments). (**c-d**) The input material from HAP1 (**c**) and HEK293T (**d**) cells (i.e. lysate prior to application to the SA beads) was immunoblotted for Prx1 (left panels) and Prx2 (right panels), demonstrating dimerization of Prx1 (left panel) and Prx2 (right panel) in response to H_2O_2. IB= immunoblot; NR = non-reducing. Blots are representatives of ≥ 3 independent experiments.

Supplementary Figure 3

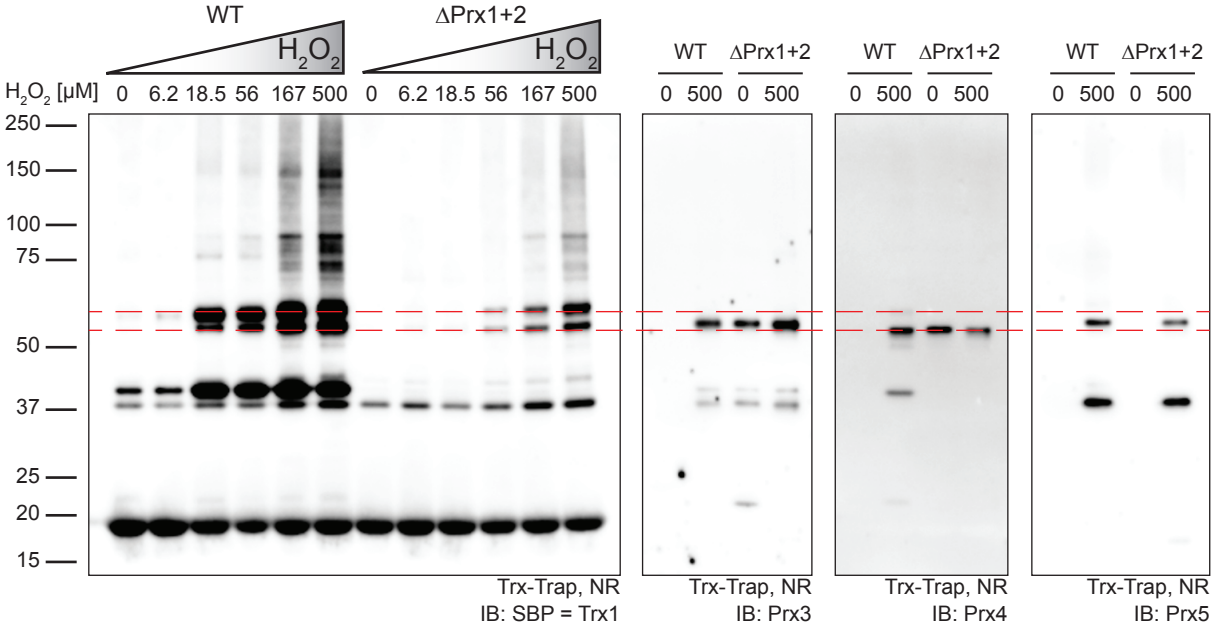

Supplementary Figure 3 | Other Prx family members contribute to the trapping pattern. HAP1 cells proficient (WT) or deficient (ΔPrx1+2) in Prx1+2 expression were treated with 500 μM H_2O_2 for 15 seconds or were left untreated. Protein thiol oxidation was then analyzed by kinetic trapping and immunoblotting against other Prx family members and compared to the pattern observed in main Fig. 1c (left panel). Immunoblotting identifies Trx conjugates of Prx3 (center left panel), Prx4 (center right panel) and Prx5 (right panel) within the size range ~55-60 kDa (dashed red lines), explaining the presence of residual Prx conjugate bands in ΔPrx1+2 cells. IB= immunoblot; NR = non-reducing; SBP= Streptavidin binding peptide. The blots are representative of ≥ 2 independent experiments.

Supplementary Figure 4

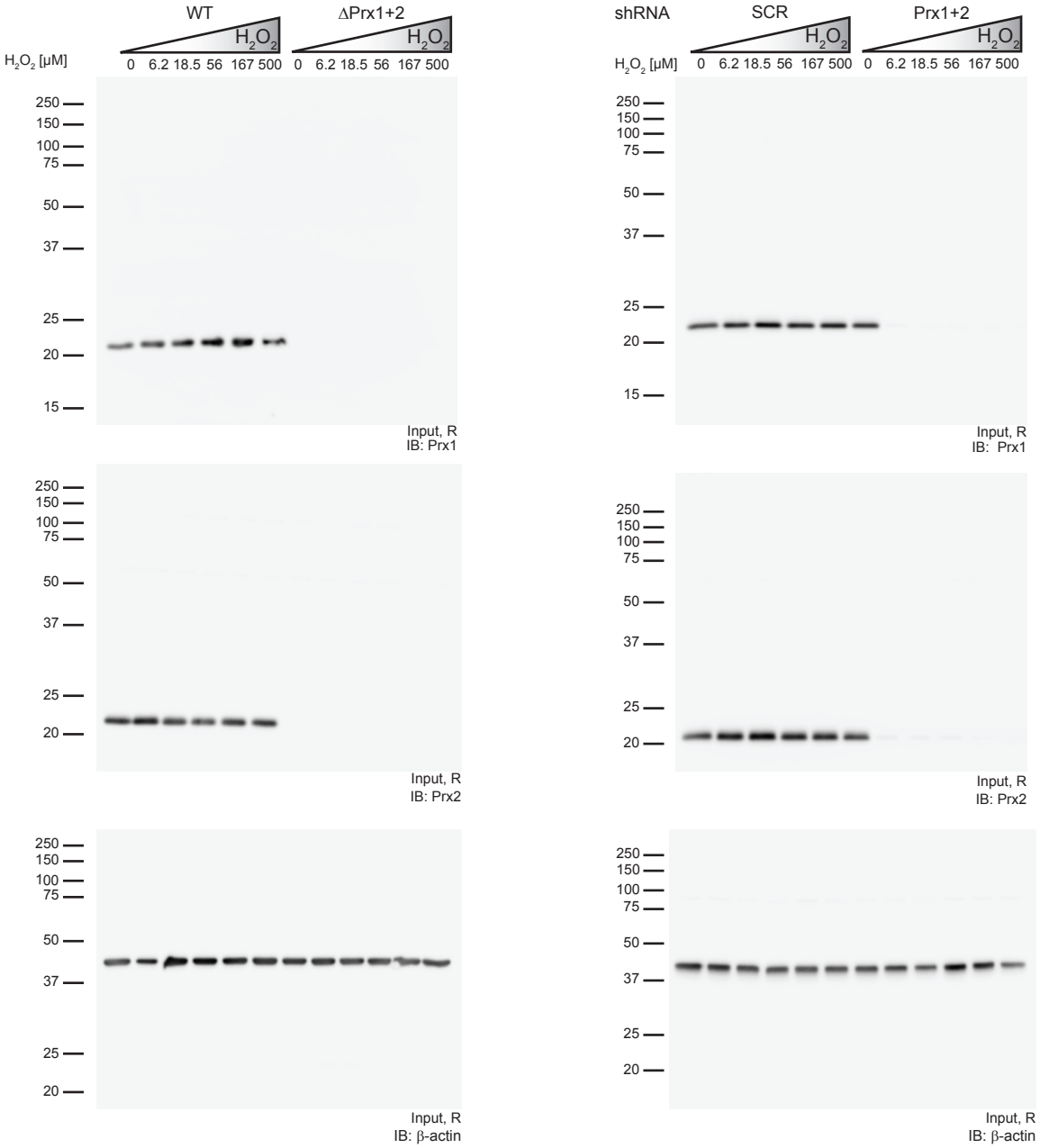

Supplementary Figure 4 | **Uncropped Blots to main figure 1**. Full size blots corresponding to the cropped Prx1, Prx2 and β-actin blots. IB= immunoblot; R = reducing. The blots are representative of ≥ 3 independent experiments.

Supplementary Figure 5

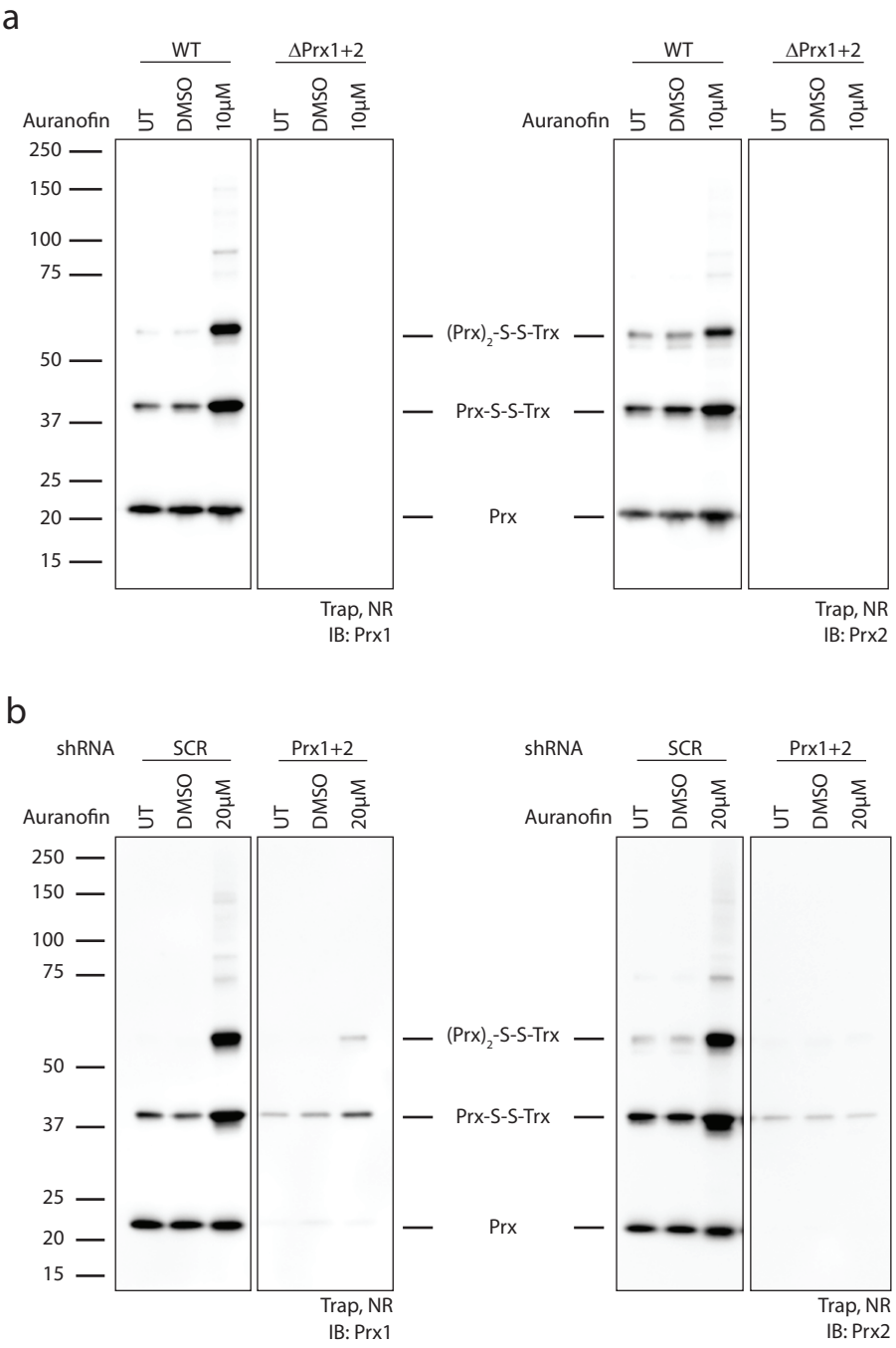

Supplementary Figure 5 | Contribution of Prx1/2 to the trapping patterns observed in main figure 2a-b. The material analyzed in main figure 2a-b (i.e. Trx(C35S) conjugates eluted with biotin from SA beads) from HEK293T (**a**) and HAP1 cells (**b**) was probed with Prx1 (left panels) and Prx2 (right panels) antibodies (on separate gels). Above immunoblots confirm that the high molecular weight bands induced by auranofin, as seen in main figures 2a-b (labelled 'Trx-S-S-X') are not (or only to minor extent) due to Trx-Prx disulfide conjugates of higher stoichiometry, and thus predominantly represent Trx(C35S) conjugated to other proteins. IB = immunoblot; NR = non-reducing; R = reducing. Blots are representative of ≥ 3 independent experiments.

Supplementary Figure 6

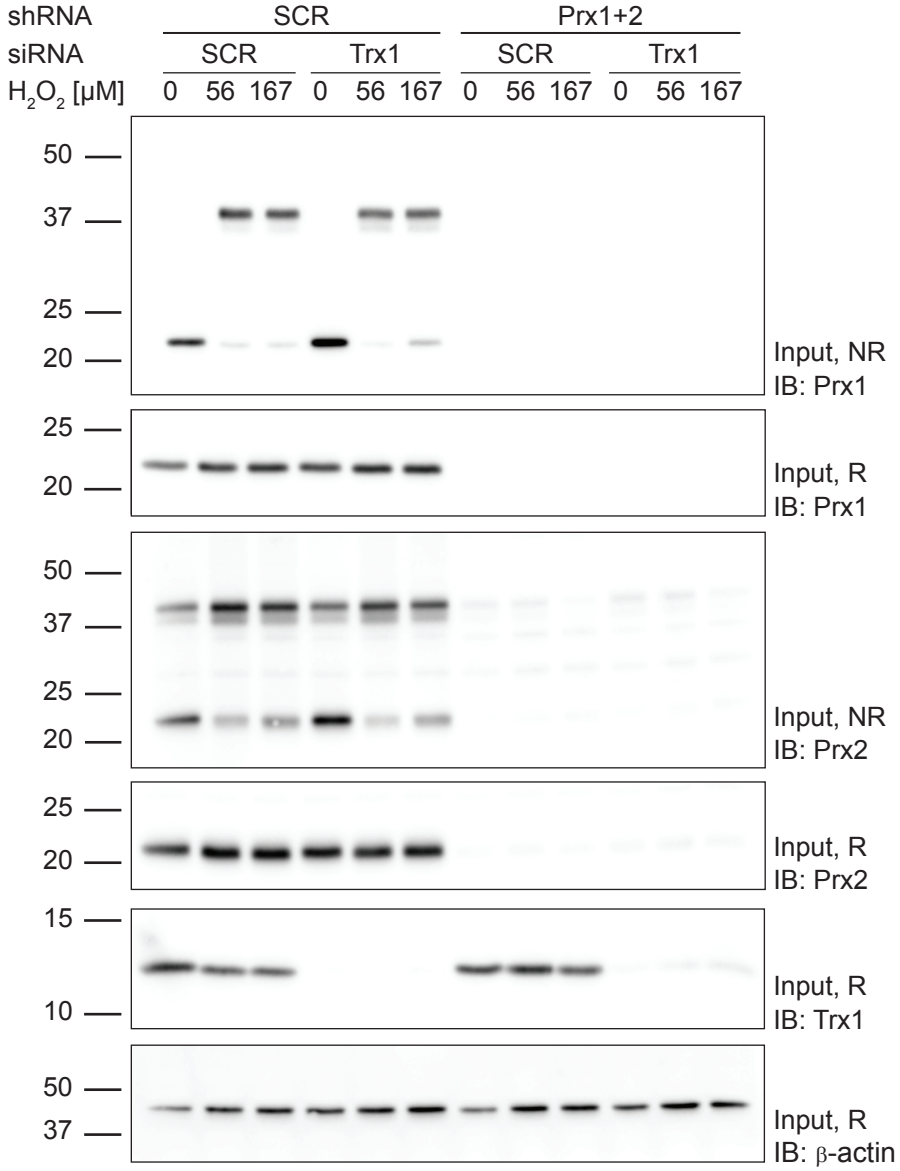

Supplementary Figure 6 | Peroxiredoxin 1 and 2 redox state is not affected by the depletion of Trx1. The input material analyzed for main figure 2c was probed with Prx1 and Prx2 antibodies. Under basal conditions Prx1 (upper panels) is in its reduced monomeric state and oxidizes (dimerizes) upon H_2O_2 treatment, independently of Trx1 expression (lower panel). Prx2 (center panels) behaves similarly, although it is already partially oxidized under basal conditions. Again, there is no detectable impact of Trx1 depletion on Prx2 redox state and oxidation behavior. IB = immunoblot; NR = non-reducing; R = reducing. The blots are representative of ≥ 2 independent experiments.

Supplementary Figure 7

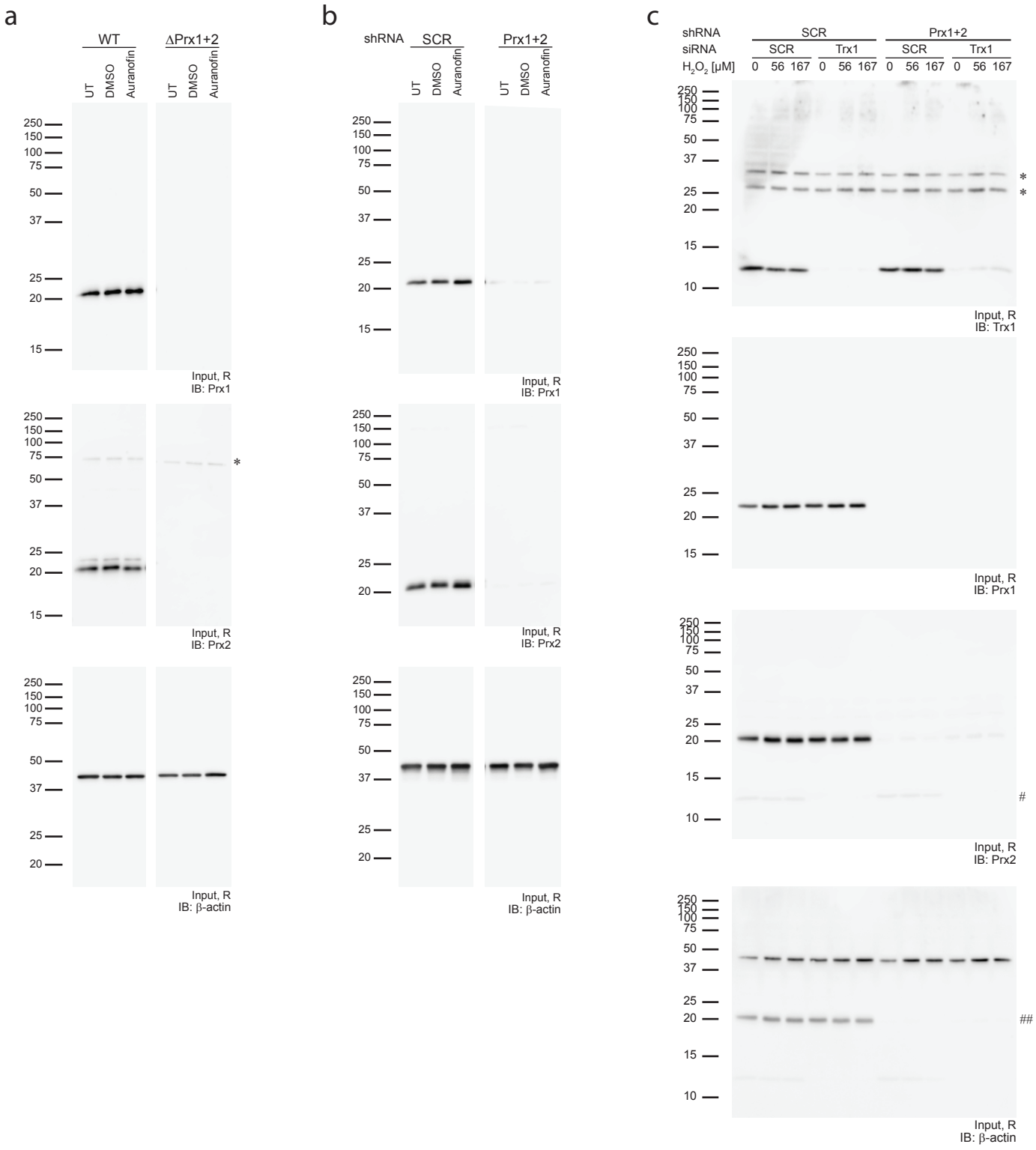

Supplementary Figure 7 | Uncropped Blots to main figure 2. (**a-c**) Full sized input blots are provided for the corresponding cropped blots shown in figure 2a (**a**), figure 2b (**b**) and in figure 2c (**c**). Bands marked with an asterisk are nonspecific bands. # and ## mark signals caused by the previous blotting of the same membrane with a different antibody (# = Trx1, ## = Prx2). IB= immunoblot; R = reducing. The blots are representative of ≥ 3 independent experiments.

Supplementary Figure 8

a

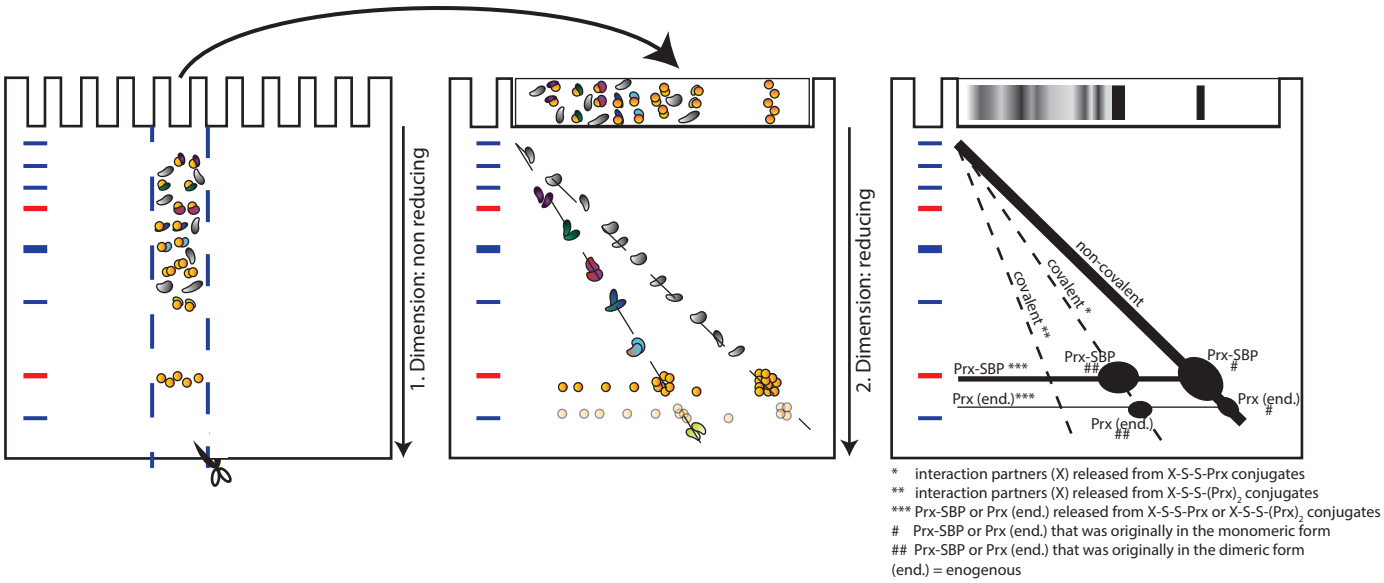

* interaction partners (X) released from X-S-S-Prx conjugates
** interaction partners (X) released from X-S-S-$(Prx)_2$ conjugates
*** Prx-SBP or Prx (end.) released from X-S-S-Prx or X-S-S-$(Prx)_2$ conjugates
\# Prx-SBP or Prx (end.) that was originally in the monomeric form
\#\# Prx-SBP or Prx (end.) that was originally in the dimeric form
(end.) = enogenous

b

Prx1

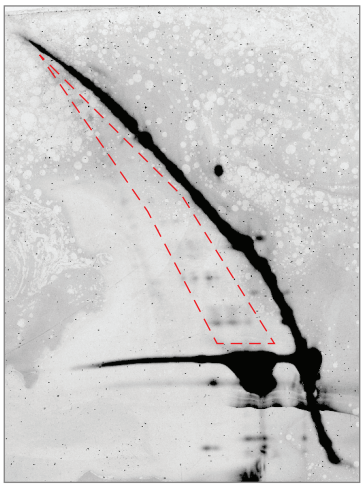

c

Prx2

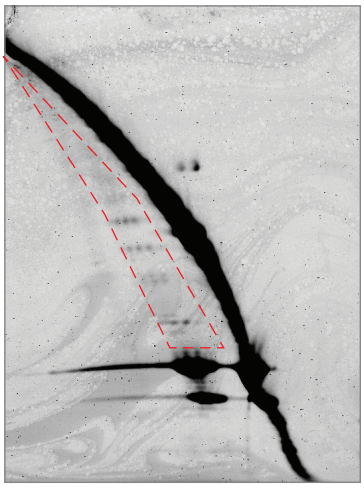

d

Prx2 ($\Delta C_P \Delta C_R$)

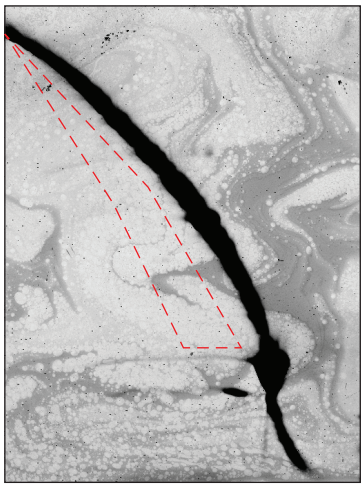

e

Trx1 (CSAAA)

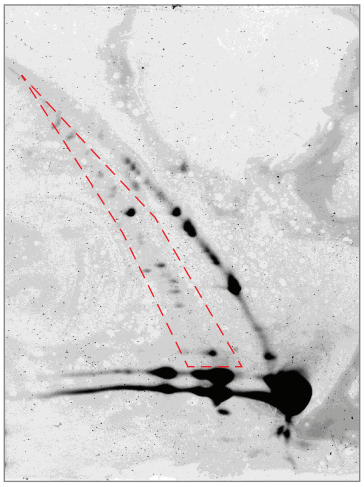

Supplementary Figure 8 | Prx1, Prx2 and Trx1 form mixed disulfide intermediates with other proteins under conditions of minimal H_2O_2 exposure (10 µM for 15 sec). (**a**) Scheme explaining two-dimensional non-reducing-reducing (diagonal) SDS-PAGE. Along the first dimension (left panel) proteins are separated under non-reducing conditions, which means that disulfide-linked proteins stay together. The excised gel slice is treated with a reductant to break apart disulfide linked conjugates. It is then placed on top of a second gel. Reduced proteins migrate along the second dimension (center panel) in relation to their mass and thereby create a distinct pattern. The right panel explains the different features of the gel. Those proteins that only interact non-covalently will settle on the main diagonal. In contrast, proteins that were covalently attached to Prx in the first dimension will run faster in the second dimension, thus settling on diagonals below the main diagonal. Here one needs to distinguish between the first lower diagonal (*) deriving from proteins that were covalently linked to a Prx monomer (X-S-S-Prx) and the second lower diagonal (**) consisting of proteins that were covalently linked to a Prx dimer (X-S-S-Prx-S-S-Prx). Prx-SBP molecules (***) liberated from covalent interactions collect along a horizontal at ~25 kDa. Endogenous Prx co-precipitates with its tagged counterpart and collects along a horizontal at ~22 kDa. Prxs that did not form disulfide bonds (#) accumulate on the main diagonal at ~25 kDa (Prx-SBP) or at ~22 kDa (wt Prx). The previously dimeric Prx (##) accumulates a bit further left at the intersection with the lower, faster migrating diagonal. (**b-d**) HEK293T cells expressing Prx1-SBP (**b**), Prx2-SBP (**c**) or Prx2($\Delta C_P \Delta C_R$)-SBP (**d**) were exposed to 10 µM H_2O_2 for 15 sec. Following thiol blocking with 100 mM NEM for 5 min, cell lysis and affinity purification, the resulting complexes were separated by 2D NR-R SDS-PAGE as described in **a**. Proteins were stained with Coomassie and imaged with an Odyssey infrared imaging system. (**e**) Immobilized recombinant trapping mutant Trx1(C35S) was allowed to interact for 1 h with the cytosolic efflux of HEK293T cells treated in the same way (10 µM H_2O_2 for 15 sec, followed by thiol blocking with 10 mM NEM for 5 min). These experiments show that even very mild and short-lived exposure to H_2O_2 leads to both Prx and Trx disulfide exchange intermediates with other proteins, but only if a catalytically active form of Prx is expressed. Regions marked by the red dashed line were excised and analyzed by mass spectrometry.

Supplementary Figure 9

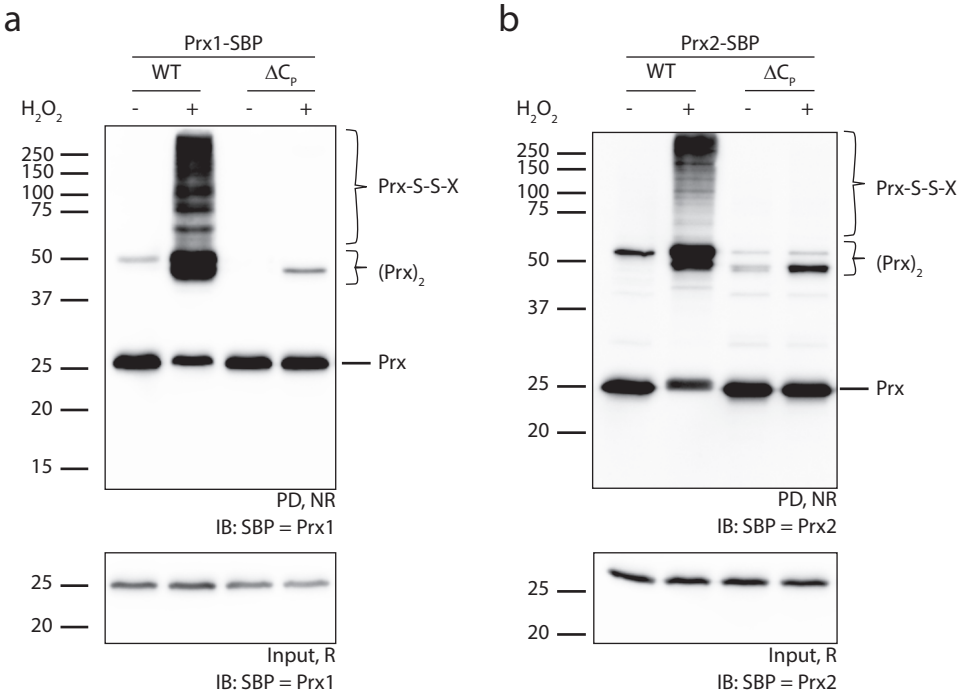

Supplementary Figure 9 | Mutation of the peroxidatic cysteine is sufficient to fully abolish the formation of covalent complexes between peroxiredoxins and other proteins. (**a-b**) HEK293T cells expressing wild type (WT) or mutant (ΔC_P) Prx1-SBP (**a**) or Prx2-SBP (**b**) were exposed to 100 µM H_2O_2 for 1 min. Following affinity purification, resulting complexes were analyzed by immunoblotting of non-reducing SDS-PAGE gels. Wild type Prx1 and Prx2, but not the respective ΔC_P mutants, form numerous Prx-S-S-X disulfide exchange intermediates in response to H_2O_2, revealing the central role of the peroxidatic cysteine for engaging in covalent interactions with other proteins. IB = immunoblot; NR = non-reducing; R = reducing; SBP = streptavidin binding peptide.

Supplementary Figure 10

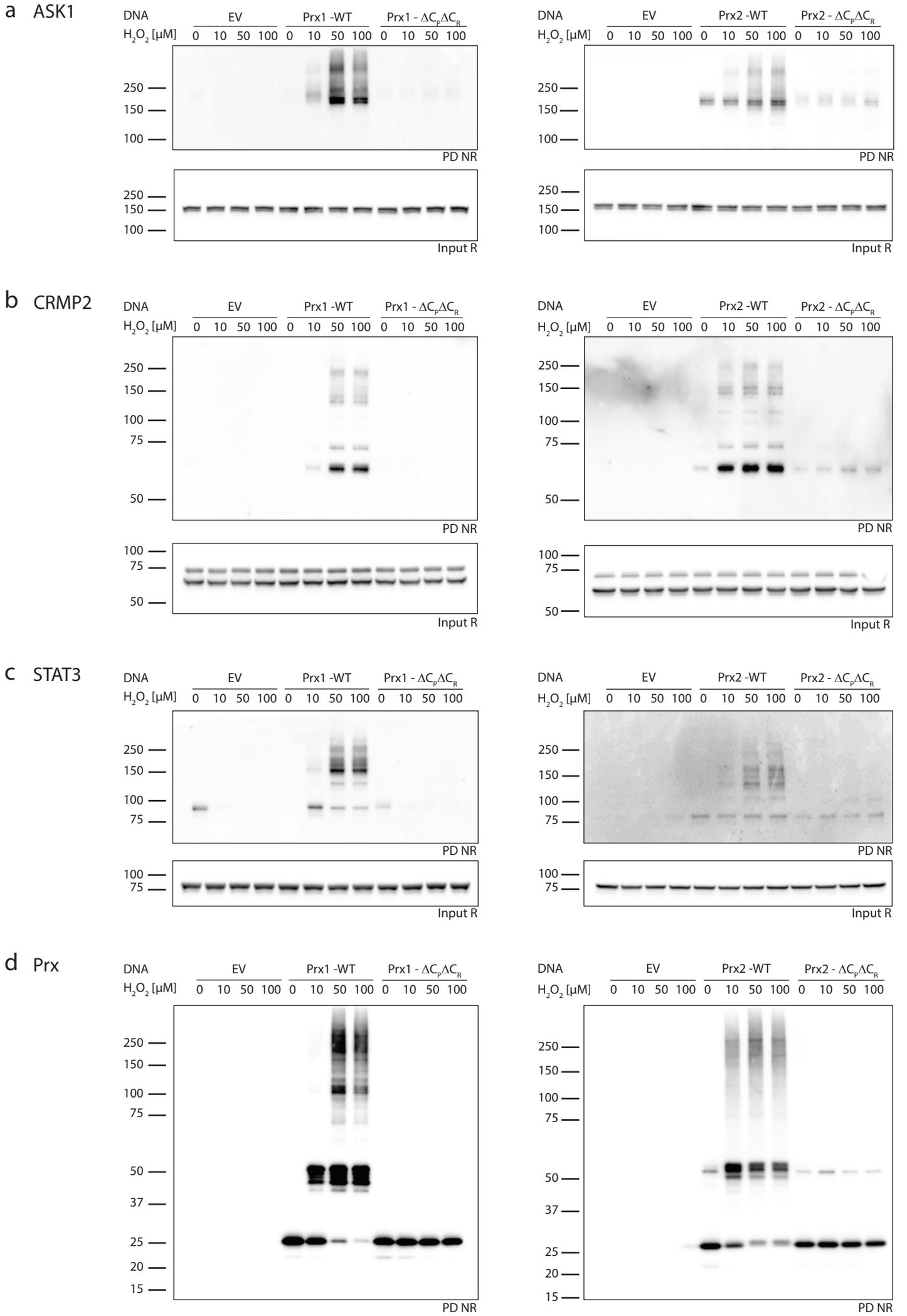

Nature Chemical Biology: doi:10.1038/nchembio.2536

Supplementary Figure 10 | Individual proteins form transient disulfide exchange intermediates with cytosolic peroxiredoxins. (**a-d**) HEK293T cells expressing tagged wild type (WT) or double mutant ($\Delta C_P \Delta C_R$) Prx1 (left panels) or Prx2 (right panels), or empty vector (EV), were treated with increasing concentrations of H_2O_2 for 1 min. Following the blocking of free thiols, cell lysis and affinity purification, conjugate formation between Prxs and ASK1 (**a**), CRMP2 (**b**) or STAT3 (**c**) was analyzed by immunoblotting. (**d**) Visualization of Prxs in the same experiment using an antibody against the SBP tag. These results confirm the covalent interaction of individual proteins with peroxiredoxins. IB = immunoblot; NR = non-reducing; R = reducing; SBP = streptavidin binding peptide. Blots are representative of 2 independent experiments each.

Supplementary Figure 11

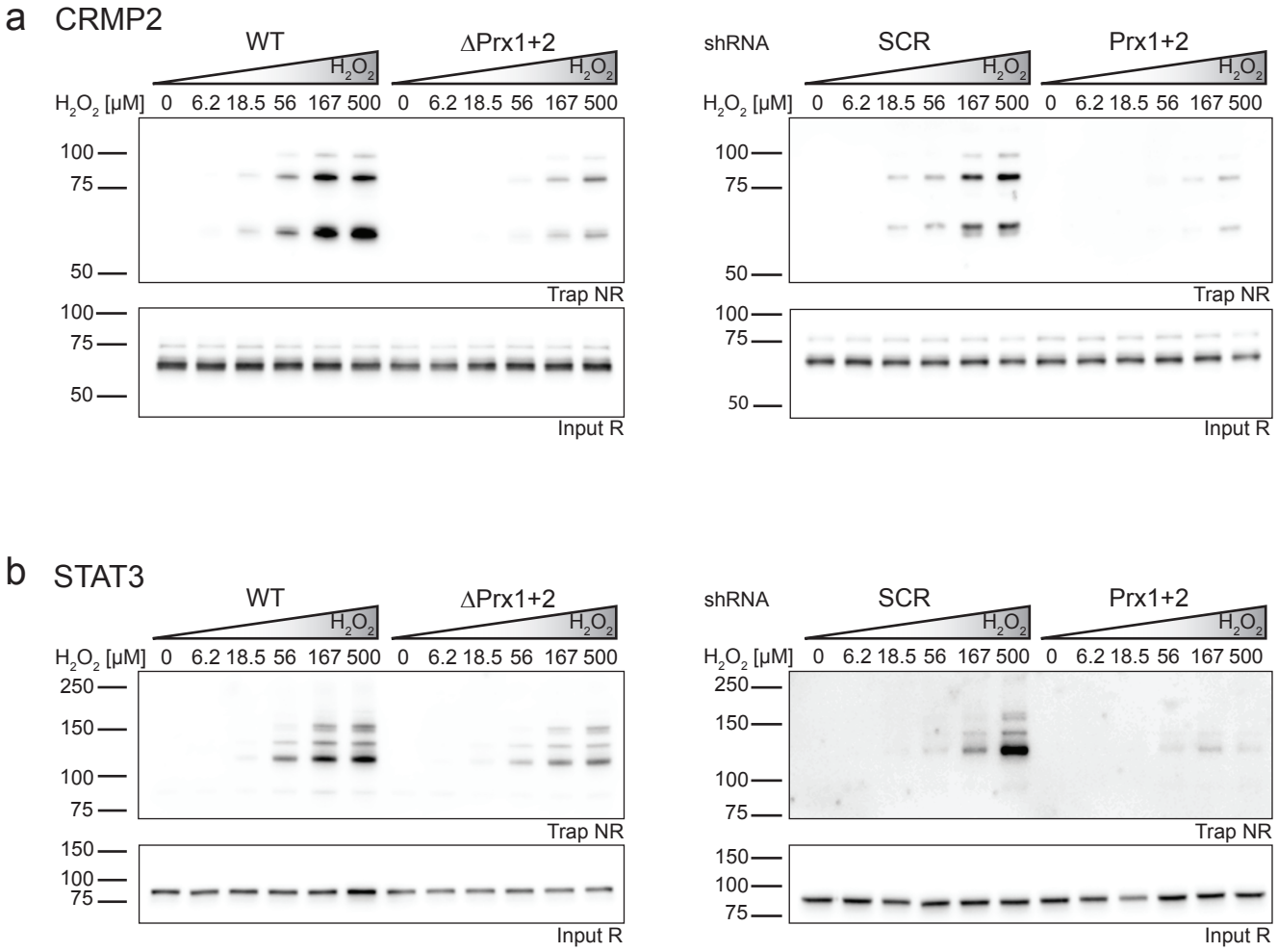

Supplementary Figure 11 | Oxidation of individual redox-regulated proteins depends on the presence of Prxs (addendum to main figure 4). (**a-b**) HAP1 cells proficient (WT) or deficient (ΔPrx1+2) in Prx1+2 expression (left panels) and HEK293T cells induced to express scrambled (SCR) or specific (Prx1+2) shRNA (right panels) were exposed to the indicated concentrations of H_2O_2 for 15 seconds. Protein thiol oxidation of CRMP2 (**a**) and STAT3 (**b**) was assessed by kinetic trapping and analyzed by immunoblotting. NR = non-reducing; R = reducing conditions. Blots are representative of ≥ 2 independent experiments.

Supplementary Figure 12

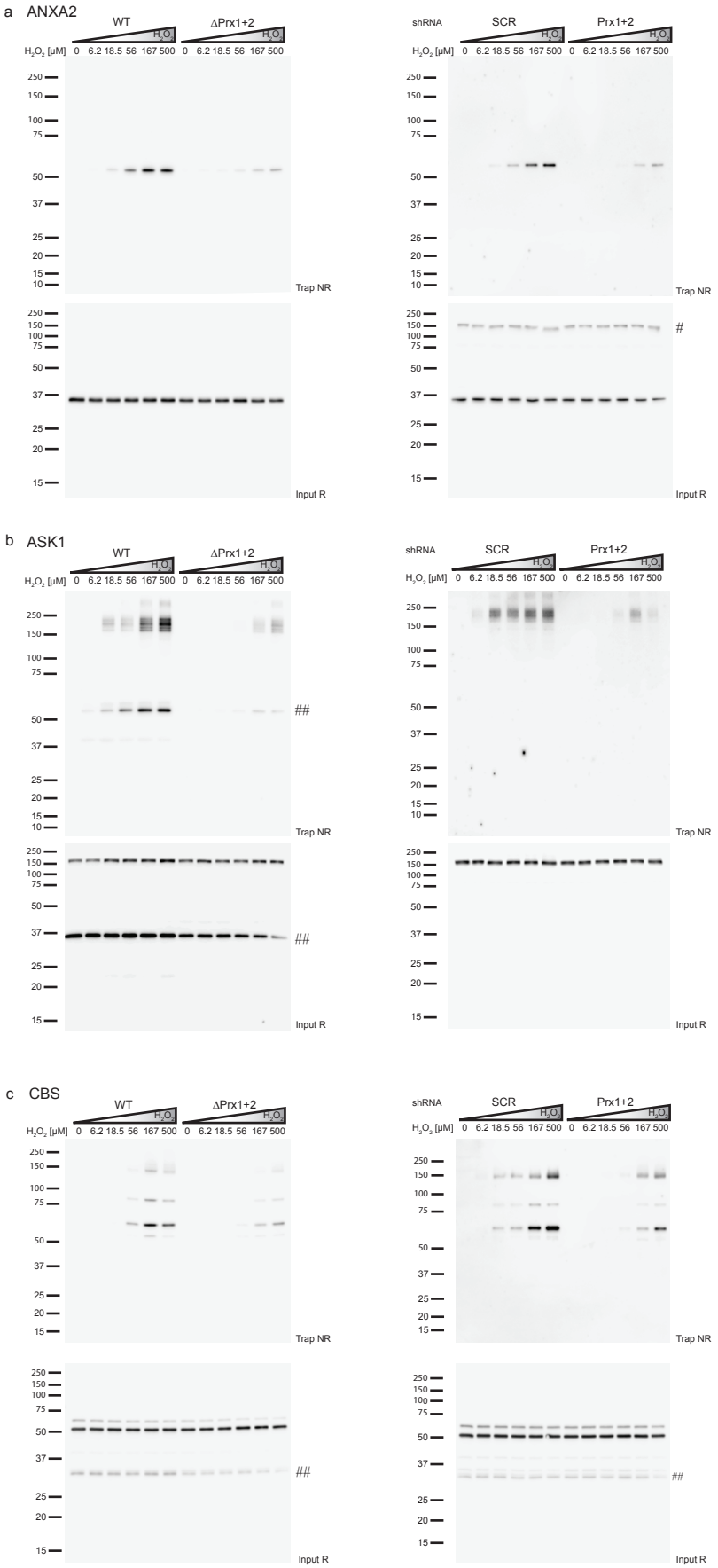

Supplementary Figure 12 | Uncropped Blots to main figure 4. (**a-c**) Full sized blots corresponding to cropped blots (ANXA2, ASK1 and CBS) for HAP1 (left panels) and HEK cells (right panels). Marked bands indicate signals caused by the previous blotting of the same membrane with a different antibody (# = ASK1, ## = ANXA2). IB= immunoblot; NR = non-reducing; R = reducing. The blots are representative of ≥ 2 independent experiments.

Supplementary Table 1 | Diagonal 2D-SDS-PAGE gels (Suppl. Fig. 8) were analyzed by mass spectrometry to identify proteins trapped by Trx1, and engaging in disulfide bonding with Prx1 and/or Prx2 upon treatment with 10 μM H_2O_2 for 15 seconds. The table only includes proteins that satisfy stringent identification criteria (see Material & Methods). The number of identified unique peptides, percentage of protein coverage and protein identification probability are listed for each protein. Further, we specifically selected proteins which are identified in covalent interactions with both Trx1 (left panel) and at least one of the cytosolic Prxs (Prx1 - center panel, Prx2 - right panel). Hence, the proteins in this list were not only identified in complex with one (or two) of the Prxs, but were also captured by the mechanism-based kinetic trapping, as would be expected for a protein that is oxidized by a Prx and subsequently reduced by Trx1. This list does not intend to provide a comprehensive list of Prx interaction partners, but rather presents examples and justifies our selection of individual proteins for further study. From the list we selected ANXA2, CBS and CRMP2 (highlighted in green) for further analysis. The lower panel (highlighted in red) shows corresponding data for STAT3 and ASK1, which were also retained for further analysis, although they did not satisfy stringent criteria, probably reflecting their lower abundance.

				Trx1 (FDR=0,0%)			Prx1 (FDR 0,0%)			Prx2 (FDR 0,0%)		
Accession Number	Uniprot	Identified Proteins	Number of Cysteines	Number of unique peptides	Protein coverage (%)	Protein Ident. Probability (%)	Number of unique peptides	Protein coverage (%)	Protein Ident. Probability (%)	Number of unique peptides	Protein coverage (%)	Protein Ident. Probability (%)
ACTB_HUMAN	P60709	Actin	6	44	52	100	24	25	100	11	35	100
ANXA2_HUMAN	P07355	Annexin A2	4	24	57	100	2	6	100	7	21	100
CBS_HUMAN	P35520	Cystathionine beta-synthase	11	12	32	100	8	10	100	7	19	100
CDK4_HUMAN	P11802	Cyclin-dependent kinase 4	4	8	30	100	2	6	100	7	32	100
DPYL2_HUMAN	Q16555	Dihydropyrimidinase-related protein 2 (CRMP2)	8	11	34	100	6	10	100	5	20	100
DREB_HUMAN	Q16643	Drebrin	8	2	5	100	5	9	100	5	14	100
EF1G_HUMAN	P26641	Elongation factor 1-gamma	6	7	17	100	4	6	100	6	14	100
EF2_HUMAN	P13639	Elongation factor 2	17	24	34	100	19	20	100	14	15	100
ENOA_HUMAN	P06733	Alpha-enolase	6	9	37	100	7	8	100	8	27	100
G3P_HUMAN	P04406	Glyceraldehyde-3-phosphate dehydrogenase (GAPDH)	3	7	16	100	8	9	100	8	30	100
G6PD_HUMAN	P11413	Glucose-6-phosphate 1-dehydrogenase	8	6	14	100	4	5	100	2	5	100
GSHR_HUMAN	P00390	Glutathione reductase	10	2	7	100	5	5	100	5	18	100
HS105_HUMAN	Q92598	Heat shock protein 105 kDa	16	9	14	100	27	32	100	26	30	100
HS90B_HUMAN	P08238	Heat shock protein HSP 90-beta	6	6	14	100	18	19	100	7	23	100
HSP7C_HUMAN	P11142	Heat shock cognate 71 kDa protein	4	12	19	100	16	14	100	18	28	100
IF4A1_HUMAN	P60842	Eukaryotic initiation factor 4A-I	4	7	24	100	7	13	100	5	15	100
ITPK1_HUMAN	Q13572	Inositol-tetrakisphosphate 1-kinase	10	2	8	100	3	5	100	2	8	100
PCBP1_HUMAN	Q15365	Poly(rC)-binding protein 1	9	5	15	100	6	13	100	5	15	100
PLST_HUMAN	P13797	Plastin-3	9	21	35	100	9	10	100	7	15	100
PRDX1_HUMAN	Q06830	Peroxiredoxin-1	4	31	44	100	194	77	100	12	50	100
PRDX2_HUMAN	P32119	Peroxiredoxin-2	3	18	53	100	69	66	100	31	73	100
RIR1_HUMAN	P23921	Ribonucleoside-diphosphate reductase large subunit	16	22	43	100	3	5	100	2	3	100
SERA_HUMAN	O43175	D-3-phosphoglycerate dehydrogenase	13	3	6	100	4	9	100	2	5	100
SPB6_HUMAN	P35237	Serpin B6	6	8	29	100	11	20	100	3	11	100
SYAC_HUMAN	P49588	Alanine--tRNA ligase	13	5	7,1	100	2	2	100	3	4	100
TBB4B_HUMAN	P68371	Tubulin beta-4B chain	8	2	33	100	3	11	100	2	28	100
TBB5_HUMAN	P07437	Tubulin beta chain	8	22	32	100	9	11	100	20	46	100
UBA1_HUMAN	P22314	Ubiquitin-like modifier-activating enzyme 1	19	3	5	100	10	14	100	3	4	100
UBP15_HUMAN	Q9Y4E8	Ubiquitin carboxyl-terminal hydrolase 15	22	2	3	100	11	11	100	4	5	100
EF1A1_HUMAN	P68104	Elongation factor 1-alpha 1	6	11	16	100	0	0	0	5	14	100
STAR7_HUMAN	Q9NQZ5	StAR-related lipid transfer protein 7	3	2	7	100	1	4	100	3	10	100
TBA1B_HUMAN	P68363	Tubulin alpha-1B chain	12	13	34	100	0	0	0	9	33	100
AIP_HUMAN	O00170	AH receptor-interacting protein	8	3	12	100	4	8	100	0	0	0
ANM1_HUMAN	Q99873	Protein arginine N-methyltransferase 1	10	5	15	100	5	7	100	0	0	0
NUCL_HUMAN	P19338	Nucleolin	1	7	10	100	3	3	100	1	1	60
PLIN3_HUMAN	O60664	Perilipin-3	3	11	33	100	7	20	100	1	6	99
RANB3_HUMAN	Q9H6Z4	Ran-binding protein 3	6	3	6	100	5	5	100	0	0	0
RSSA_HUMAN	P08865	40S ribosomal protein SA	2	5	17	100	6	13	100	0	0	0
THIO_HUMAN	P00390	Thioredoxin	10	9	34	100	5	31	100	1	9	63
TOPK_HUMAN	Q96KB5	Lymphokine-activated killer T-cell-originated protein kinase	6	2	8	100	7	14	100	1	3	99
STAT3_HUMAN	P40763	Signal transducer and activator of transcription 3	14	1	3	48	5	7	100	1	3	100
M3K5_HUMAN	Q99683	Mitogen-activated protein kinase kinase kinase 5 (ASK1)	23	1	2	74	1	2	72	0	0	0